From ID-TIMS U-Pb dating of single monazite grain to APT-nanogeochronology: application to the UHT granulites of Andriamena (North-Central Madagascar)

M J Turuani, A-M Seydoux-Guillaume, A T Laurent, D Fougerouse, S L Harley, S M Reddy, Philippe Goncalves, D W Saxey, J Michaud, J-M Montel, et al.

BSGF - Earth Sciences Bulletin 2024, 195, 18
© M.J. Turuani *et al.*, Published by EDP Sciences 2024
https://doi.org/10.1051/bsgf/2024013

BSGF Earth Sciences Bulletin

Available online at:
www.bsgf.fr

Special Issue Some applications of LA-ICP-MS U-Pb geochronology: A tribute to Jean Louis Paquette Marc Poujol, Valérie Bosse and Dave Chew (Guest Editors)

OPEN ACCESS

From ID-TIMS U-Pb dating of single monazite grain to APT-nanogeochronology: application to the UHT granulites of Andriamena (North-Central Madagascar)

M.J. Turuani[1,*], A.-M. Seydoux-Guillaume[1], A.T. Laurent[1], D. Fougerouse[2,3], S.L. Harley[4], S.M. Reddy[2,3], P. Goncalves[5], D.W. Saxey[3], J. Michaud[6], J.-M. Montel[7], C. Nicollet[8] and J.-L. Paquette[8,†]

[1] UJM-Saint-Etienne, CNRS, LGL-TPE, F-42023, Saint Etienne, France
[2] School of Earth and Planetary Sciences, Curtin University, Perth, Western Australia 6845, Australia
[3] Geoscience Atom Probe, John de Laeter Centre, Curtin University, Perth, Western Australia 6845, Australia
[4] School of Geosciences, University of Edinburgh, Edinburgh EH9 3FE, UK
[5] Laboratoire Chrono-environnement, Université de Franche-Comté, CNRS, 25000 Besançon, France
[6] University of Hannover, Callinstraße 3, 30167 Hannover
[7] Ecole Nationale Supérieure de Géologie, Université de Lorraine, CNRS, CRPG, F-54000 Nancy, France
[8] Laboratoire Magmas et Volcans, Université Clermont Auvergne, CNRS, IRD, OPGC, Clermont-Ferrand, France

Received: 22 December 2023/ Accepted: 4 June 2024 / Publishing online: 7 October 2024

Abstract – The causes of U-Pb isotopic discordance documented by Paquette *et al.* (2004) in monazite grains from the ultra-high temperature (UHT) granulite of the Andriamena unit of Madagascar are re-evaluated in the light of nanoscale crystal-chemical characterization utilising Atom Probe Tomography (APT) and state-of-the-art Scanning Transmission Electron Microscopy (STEM). APT provides isotopic ($^{208}Pb/^{232}Th$) dating and information on the chemical segregation of trace elements (*e.g.*, Pb) in monazite at nanoscale. Latest generation of STEM allows complementary high-resolution chemical and structural characterization at nanoscale. *In situ* isotopic U–Pb dating with Secondary Ion Mass Spectrometry (SIMS) on 25 monazite grains and Laser Ablation Inductively Coupled Plasma Mass Spectrometry (LA-ICP-MS) on zircon have been employed to refine the age spectra. Monazite and zircon grains located in quartz and garnet formed with the peak UHT metamorphic assemblage, which is partially overprinted by retrograde coronitic textures. Zircon grains hosted in garnet and in quartz yield concordant U–Pb ages at 2758 ± 28 Ma and 2609 ± 51 Ma, respectively whereas monazite grains hosted in quartz and garnet show a discordant Pb^* loss trend on the Concordia diagram recording disturbance at 1053 ± 246 Ma that is not seen by the zircon, underlining the importance of combining the use of monazite and zircon to understand the history of polymetamorphic rocks. The Pb^*-loss trend of monazite is related to petrographic position, with less Pb^* lost from monazite hosted in quartz and garnet than monazite hosted in the coronitic reaction texture domains. STEM shows that the garnet- and quartz-hosted monazite grains contain more Pb-bearing nanophases than monazite grains located in the coronitic textures. An inverse correlation between the number of Pb-bearing nanophases and the percentage of Pb^*-loss in monazite grains demonstrates that Pb^* is retained in the grain in the form of nanophases. The formation of Pb-bearing nanophases limits Pb^*-loss at the grain scale and therefore allows the preservation of early events. $^{208}Pb/^{232}Th$ ratios obtained with APT in monazite located in quartz and garnet and excluding Pb^*-bearing nanophases indicate a mean age of 1059 ± 129 Ma corresponding to a disturbance event *hitherto* undetected in the geochronological record of the Andriamena unit. Thus, geochronology with APT allows access to information and the definition of events that may be blurred or obscured when examined at lower spatial resolution.

Keywords: Monazite / Andriamena unit (Madagascar) / U-Th-Pb isotopic disturbance / atom probe tomography / Pb-bearing nanophases

*e-mail: marion.turuani@univ-grenoble-alpes.fr
†Deceased in June 2022

1 Introduction

In geochronology, the significance and geological interpretation of dates remain a major question despite the major analytical developments of the past 20 yr. In monazite and zircon, which are extensively used in geochronology, the intracrystalline mobility of uranium, thorium and lead, from nanometer to micrometer distances, can impact geochronological results. The distribution of U, Th and Pb has been investigated at a nanoscale with transmission electron microscopy (TEM) in monazite (Seydoux-Guillaume *et al.*, 2003; Hyde *et al.*, 2024) and zircon (Utsunomiya *et al.*, 2004; Kusiak *et al.*, 2015; Seydoux-Guillaume *et al.*, 2015; Whitehouse *et al.*, 2017) from ancient and polymetamorphic settings. Over the past decade, atom probe tomography (APT) has allowed nanoscale isotopic investigations in geochronometers (zircon: Valley *et al.*, 2014; Peterman *et al.*, 2016; Piazolo *et al.*, 2016, monazite: Fougerouse *et al.*, 2018, Fougerouse *et al.*, 2021a, baddeleyite: White *et al.*, 2017 and rutile: Verberne *et al.*, 2020) and some studies have applied both of these two highly complementary methods in geochronometers (monazite: Seydoux-Guillaume *et al.*, 2019; Fougerouse *et al.*, 2021b; Turuani *et al.*, 2022, Turuani *et al.*, 2023 Verberne *et al.*, 2023). These studies have highlighted the presence of nanoscale Pb-bearing features (*i.e.*, clusters and nanophases) and demonstrated the need for characterization at high spatial resolution coupled with *in situ* U-Th-Pb micrometer scale dating (for example with laser ablation inductively coupled plasma mass spectrometry, LA-ICP-MS), for dating geological events such as metamorphism (Seydoux-Guillaume *et al.*, 2019; Turuani *et al.*, 2022) or bolide impacts (Hyde *et al.*, 2024). Such Pb-bearing nanofeatures are mainly found in monazite and zircon present in Archean cratonic rocks, which record ancient geological histories (Gyrs). These prolonged evolutions result in the accumulation of considerable radiogenic Pb (Pb^*), up to more than one weight percent in the mineral geochronometer. Under the imposition of secondary metamorphic episodes, Pb^* accumulated in a geochronometer can be redistributed over the time when the system remains open. Some of the Pb^* remains trapped within the parent (host) grain in the form of Pb^*-bearing nanophases resulting in "fossil" Pb-reservoirs and some of the Pb^* escapes into the metamorphic media (*e.g.*, fluid phase) to be subsequently redistributed among other minerals acting as Pb-sinks (*e.g.*, feldspars). The presence of Pb^*-bearing nanofeatures, which has been mostly regarded as a drawback by geochronologists, may instead carry unique geochronological information that is unable to be accessed at the microscale. To evaluate the positive and negative impacts of these Pb^*-bearing nanofeatures for microscale geochronology it is essential to document their mineralogy and composition and thereby evaluate the particular P-T-fluid conditions under which they form.

In this contribution, we reinvestigate the U-Pb record of monazite in a Neoarchean granulite rock-sample (An6e), where unusual U–Pb discordance and Pb mobility in monazite has been documented (Seydoux-Guillaume *et al.*, 2003; Paquette *et al.*, 2004). New micro to nanoscale observations and isotopic analyses using advanced analytical instrumentation (TEM and APT) are combined to document the scales and mechanisms of this Pb mobility and the resulting mineralogical features. The consequences on microscale geochronology carried out at various spatial resolutions using ID-TIMS, LA-ICP-MS, SIMS and EPMA are evaluated. Finally, monazite U-Pb data are compared with zircon U-Pb data from the same sample to highlight the complementarity of both geochronometers in deciphering the polycyclic history of Archean high-grade rocks.

2 Geological background

Located in the north centre of Madagascar, the Andriamena unit is mostly composed of mafic gneisses and migmatitic metapelites (Fig. 1a). The unit is a part of the Tsaratanana complex, which is considered as an allochton on the Antananarivo unit (Fig. 1a). The area has been involved in successive continental amalgamation from Neoarchean to Cambrian. Rocks from Andriamena record Neoarchean dates of ~2.7 Ga obtained from discordant zircon and monazite, which may correspond to the protolith age or to an unresolved metamorphic event (Paquette *et al.*, 2004; Kabete *et al.*, 2006). The oldest undisputed metamorphic event, dated at ~2.5 Ga, reached ultra-high temperature (UHT) conditions of 1050 ± 50 °C and 11.5 ± 1.5 kbar (Goncalves *et al.*, 2004; Paquette *et al.*, 2004; Kabete *et al.*, 2006). The second major thermal event to affect these rocks (850–900 °C and 7 kbar) occurred at ~790 Ma (Goncalves *et al.*, 2004; Paquette *et al.*, 2004). That event was associated with intense coeval magmatism (Guerrot *et al.*, 1993; Handke *et al.*, 1999; Tucker *et al.*, 1999; Kröner *et al.*, 2000; Bybee *et al.*, 2010; Boger *et al.*, 2014, 2015; Archibald *et al.*, 2016, 2017; Armistead 2019) including the emplacement of numerous mafic to ultramafic massifs (Fig. 1a; Guerrot *et al.*, 1993; Bybee *et al.*, 2010). The last significant metamorphic event occurred under amphibolite facies conditions (650-700 °C and 5-7 kbar; Goncalves *et al.*, 2003) during the Cambrian (530-500 Ma). This event was associated with granite intrusions and is considered to reflect Gondwana amalgamation (Martelat *et al.*, 2000; Goncalves *et al.*, 2003; Tucker *et al.*, 2014; Tang *et al.*, 2018). Although the late Archean (~2.5 Ga), late Proterozoic (~790 Ma) and Cambrian (530-500 Ma) events are well constrained by geochronometers and reported elsewhere in Madagascar (Goncalves 2002; Goncalves *et al.*, 2003, 2004, 2005; Paquette *et al.*, 2004), the Neoarchean record (~2.7 Ga) is still obscure.

3 Previous studies

3.1 Petrographic description

An6e is a granulite collected in the Andriamena unit, near Brieville (Fig. 1a). The sample contains garnet, orthopyroxene, sillimanite and abundant quartz corresponding to the UHT peak metamorphic assemblage formed during the late Archean at ~2.5 Ga (Nicollet 1988; Goncalves *et al.*, 2004). A secondary mineral assemblage composed of orthoamphibole, cordierite and biotite is developed at the expense of garnet and quartz as coronitic textures (Fig. 1b). This retrogression is interpreted as the result of near isobaric cooling from 7-8 kbar and 900 °C to ~5 kbar and 650 °C at ~790 Ma (Goncalves

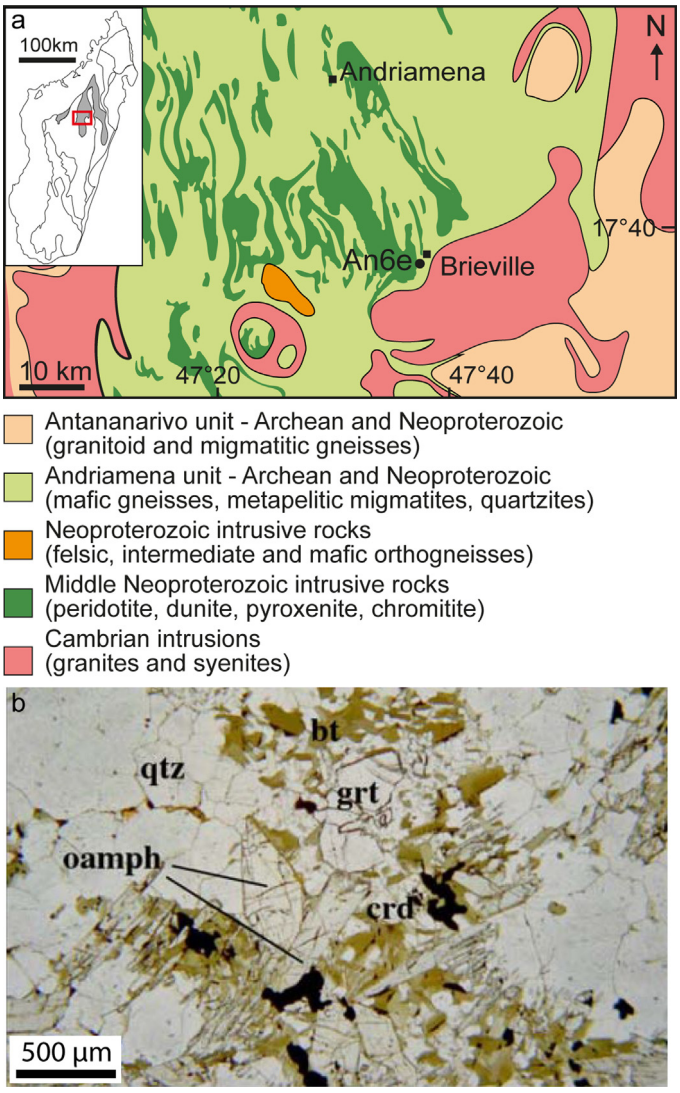

Fig. 1. a: simplified geological map of the interest area and An6e sample location, compile from Goncalves *et al.* (2003), Rasolomanana *et al.* (2010), Nédelec *et al.* (2016) and Archibald *et al.* (2016). Insert showing the location of Tsaratana complex in grey. b: photomicrograph of An6e showing primary garnet and quartz and the secondary coronitic texture composed of ortho-amphibole, cordierite and biotite. (modified from Goncalves, 2002). Bt = biotite, crd = cordierite, grt = garnet, oamph = orthoamphibole, qtz = quartz.

et al., 2004). The last event reported in Andriamena unit at 530-500 Ma (Goncalves *et al.*, 2003) has led to the formation of recrystallized domains in monazite grains from An6e (Paquette *et al.*, 2004; Goncalves *et al.*, 2005). Garnet in the same rocks show low-Y overgrowths that are inferred to reflect a second stage of growth following partial resorption of the initial garnet. It is considered that garnet which crystallized at ~2.5 Ga was destabilized at ~790 Ma, reacting to form cordierite and orthoamphibole (reaction: Gt+Q+V=Cord+Oamph), and then marginally regrowing through the reverse reaction to form a new Y-low generation.

Monazite and zircon grains are located in quartz, garnet or in the coronitic texture. Monazite grains present homogeneous core (1), some grains present a second distinct chemical domain (2) independently of the petrographic position and all monazite grains present recrystallized domains and overgrowths (3) which are more abundant in monazite located in the coronitic texture and may occur as rims or discontinuous domains (Goncalves 2002; Goncalves *et al.*, 2005; Paquette *et al.*, 2004). Monazite grains located in coronitic textures have very irregular morphologies due to their intergrowth with orthoamphibole and biotite and abundant euhedral inclusions of quartz and biotite within them. These textural observations led Paquette *et al.* (2004) to suggest that monazite in these domains was affected by partial dissolution and reprecipitation coeval with the crystallization of orthoamphibole and biotite that was associated with garnet retrogression at ~790 Ma.

Monazite chemical compositions vary according to their petrographic position, shape, and size. Goncalves (2002) highlights 3 compositional groups: (1) the "UHT group", exhibits a homogeneous composition dominated by huttonite cation substitution ($Si^{4+} + Th^{4+} = P^{5+} + LREE^{3+}$) and corresponds to monazite grains included in garnet, and to homogeneous cores, (2) the "low grade group" displays composition variation following the huttonite substitution and corresponds to monazite located in quartz or coronitic texture,

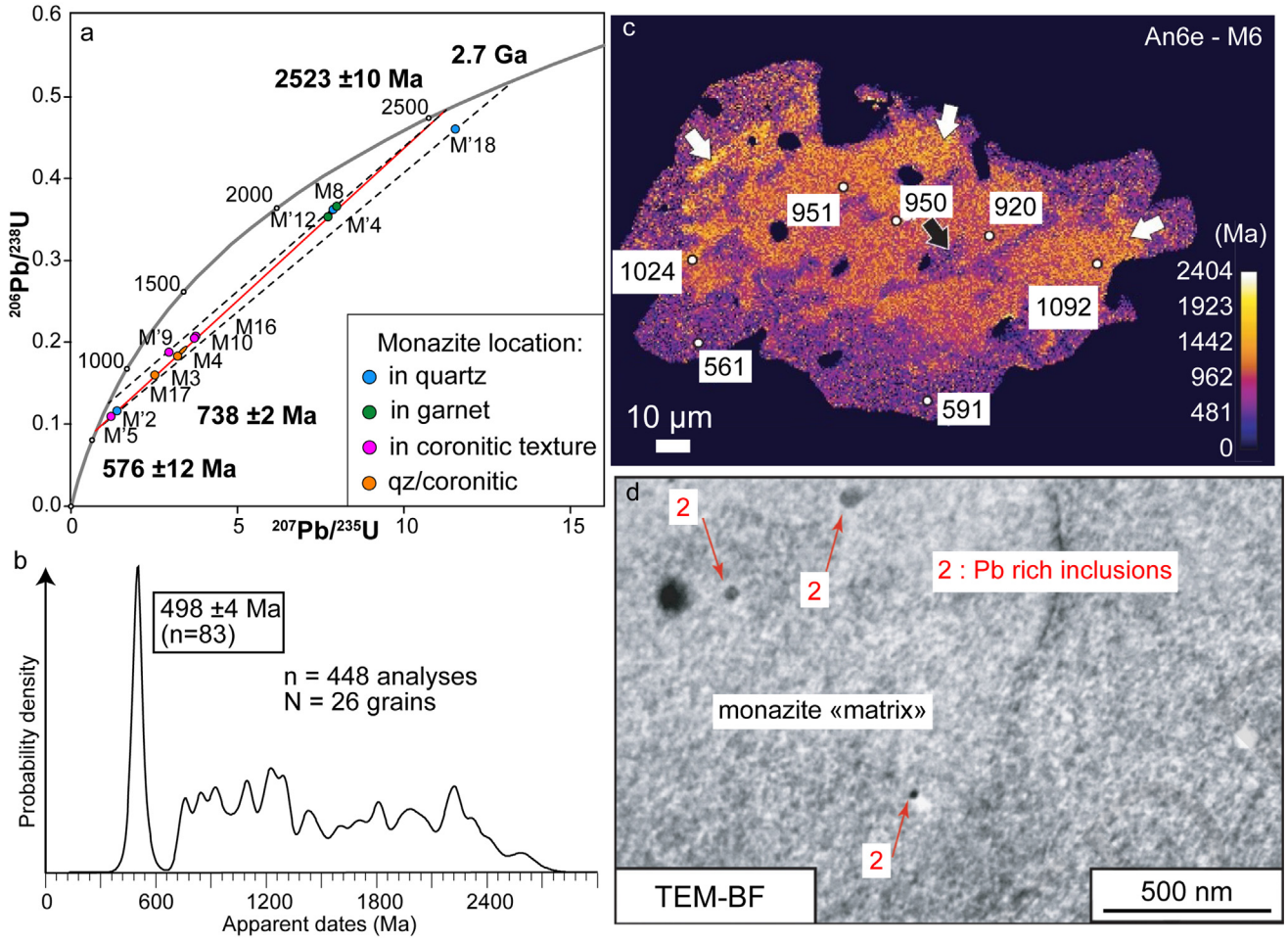

Fig. 2. Previous studies on monazite from An6e. a: ID-TIMS results obtained on An6e monazite grains, where one analysis point corresponds to one monazite grain, and showing complex discordance of monazite. Modified from Paquette *et al.* (2004). b: EMP dating results on An6e monazite grains showing a statistically well constrained date at 498 ± 4 Ma and a large dispersion between 2700 Ma and 700 Ma. Modified from Goncalves, (2002). c: Age map of monazite M6 in An6e with EMP *in situ* dates (white dots). Purple domains corresponds to the young domains while orange domains correspond to the oldest dates (white arrows). Modified from Goncalves *et al.* (2005). d: TEM-BF imaging on An6e monazite grain showing the presence of Pb rich inclusions. Modified from Seydoux-Guillaume *et al.* (2003).

(3) the third group, the "Cambrian group", is represented by outermost recrystallized domains and overgrowths with a composition dominated by the cheralite substitution ($Ca^{2+} + Th^{4+} = 2LREE^{3+}$).

3.2 Geochronological data and open questions

Isotopic data obtained from isotope dilution thermal ionization mass spectrometry (ID-TIMS) and electron-microprobe (EMP) dating on monazite have been published by Paquette *et al.* (2004; Fig. 2a and 2b). This dataset is outstanding because (1) each isotopic analysis point corresponds to a single grain of monazite that was extracted by micro-drilling directly from the thin-section, thereby preserving the textural setting of the analysis; and (2) each grain was dated *in situ* by EMP chemical dating (Fig. 2b). Monazite ID-TIMS dates show extensive dispersal and discordance, which is unusual for monazite. Ten out of twelve analyses define a Discordia with an upper intercept at 2523 ± 10 Ma, an age that corresponds to the well constrained UHT event in the area. In contrast, the lower intercepts obtained from ID-TIMS, 738 ± 2 Ma and 576 ± 12 Ma do not match particularly well with the 790 Ma and 530-500 Ma Cambrian regional events recorded in other samples (Paquette *et al.*, 2004). These significant mismatches have been interpreted by Paquette et al. (2004) to result from the mixing of different age domains in monazite grains, highlighted by EMP chemical age maps which show the internal variations in individual monazites (Fig. 1c; Goncalves *et al.*, 2005). The Cambrian event is however well defined by EMP dating of monazite in the third chemical domain "Cambrian group" yielding an unimodal date of 498 ± 4 Ma (Fig. 2b; Goncalves 2002; Paquette *et al.*, 2004). The oldest age that was inferred from the ID-TIMS monazite dataset in an upper intercept around 2.7 Ga loosely defined by a Discordia passing through the monazite with oldest $^{206}Pb/^{238}U$ apparent age and anchored at 576 ± 12 Ma (lower intercept). A similar 2.71 Ga age has been measured by U-Pb ID-TIMS on zircon retrieved from samples belonging to the same geological unit (2705 ± 1 Ma in sample C1 and 2709 ± 4 Ma

in sample C43; Paquette *et al.*, 2004) and has been interpreted as the protolith emplacement age.

The causes of this unusual and unresolved discordance in the monazite ID-TIMS dataset has been explored with TEM by Seydoux-Guillaume *et al.* (2003). A monazite grain located in quartz revealed the presence of Pb-bearing features less than 100 nm in diameter (Fig. 2d). These features show high content in Pb, Ca and Si and were interpreted as probable fluid inclusions or as a crystalline phase such as margarosanite ($Ca_2PbSi_3O_9$) or Pb-cheralite [$PbTh(PO_4)_2$] (Seydoux-Guillaume *et al.*, 2003). While it was clear that those inclusions were likely to be central to developing and understanding of the unusual discordance pattern observed in the ID-TIMS geochronology, it was not possible at the time to assess their nature nor their quantitative impact on U-Pb isotopic systematics.

4 Methods

Monazite crystals were observed using a field emission gun scanning electron microscopy (SEM-FEG) Zeiss supra 55vp, equipped with energy dispersive spectroscopy (EDS) and back scattered electron (BSE) detectors. The instrument is hosted at the *Ecole Normale Supérieure* in Lyon (France).

Secondary Ions Mass Spectrometry (SIMS) was carried out *in situ* on monazite grains in thin section, using the Cameca ims-1270 ion microprobe at the Edinburgh Ion Microprobe Facility (EIMF) in the School of GeoSciences, University of Edinburgh. Prior to analysis, the thin sections and inserted standards were imaged using transmitted and reflected light microscopes and a Phillips XL30 Scanning Electron Microscope (SEM). Monazite U-Th-Pb SIMS analysis followed similar procedures to those described by Harley & Nandakumar (2014). Common lead corrections were based on counts at mass 204 corrected for interferences and assuming modern lead. Correction of Pb/U ratios for instrument drift over the analysis period was made using the relationship between Ln(Pb/U) and Ln(UO_2/UO). The effect of the production of excess ^{206}Pb from the decay of ^{230}Th within high-Th monazite was accounted for using a fractionation factor f [(Th/U)monazite/(Th/U)melt] of 30, applied to the monazite standard and unknowns. This results in a 0.6% correction to the ^{207}Pb/^{206}Pb ratios, which is propagated into the final ^{206}Pb/^{238}U ratios used in age calculations. Analyses were referenced against *in situ*, within sample, analyses of the Moacyr standard (provided by J.-M. Montel), for which 9 analyses bracketing the 13 analyses of An6e unknowns gave an average corrected ^{206}Pb/^{238}U ratio of 0.0815 ± 0.0030, which corresponds to a ^{206}Pb/^{238}U age of 505 ± 17 Ma (2σ; MSWD = 0.7). The large uncertainty arises because of unavoidable irregularities in the polished sample surface of An6e but the average result is consistent with the ID-TIMS ^{207}Pb/^{235}U age of 504.3 ± 0.2 Ma reported by Gasquet *et al.* (2010) for Moacyr. The monazite data were reduced online using in-house data reduction spreadsheets and subsequently processed for age statistics and fits using the online version of IsoplotR (Ludwig, 2003; Vermeesch, 2018). Uncertainties on ages quoted in the text and in tables for *individual analyses* ratios and ages are at the 1σ and 2σ level respectively. All uncertainties in calculated *group* ages are reported at 95% confidence limits. Concordia diagrams were calculated with ^{206}Pb/^{238}U and ^{207}Pb/^{235}U ratios corrected for a generally very minor common Pb component as calculated from measured ^{204}Pb.

LA-ICP-MS analyses were undertaken on zircon using an ICP-MS quadripole Agilent 7500cs hosted at *Laboratoire Magmas et Volcans* (Clermont-Ferrand, France). The laser excimer system is a Resonetics M-50E. The laser ATL has a wavelength of 193 nm, a frequency of 3 Hz. The spot diameter of 20 μm was used for analyses. Zircon standard GJ-1 (Jackson *et al.*, 2004) was used to correct elementary fractionation and U, Th and Pb calibration. Glitter software was used for processing data.

Samples for TEM were prepared using a Thermo Fisher Scientific FEI Helios Nanolab 600i focused-ion beam (FIB-SEM) hosted by MANUTECH USD platform in Saint-Etienne (France). Two FIB foils were prepared in monazite M6 located in the recrystallized coronitic texture (FIB-foils location Fig. 3e) and two were prepared in monazite M15 located in garnet (FIB-foils location Fig. 3a). One FIB foil was extracted from M13 monazite located in a quartz (FIB-foil location Fig. 3c) and has been prepared and studied in a previous study where details of preparation method are reported (Seydoux-Guillaume *et al.*, 2003). Contrary to FIB foils prepared for the present study (from M6 and M15) which are fixed on half copper-grid, the FIB foil from M13 is deposited on carbon coated copper-grid.

A Tescan Lyra3 Ga^+ FIB-SEM housed at Curtin University was used to prepare six needle-shaped APT specimens following established protocols (Rickard *et al.*, 2020). Two specimens (3263 and 3273) targeted the core of monazite M13 (location Fig. 3c), one (14126) from the core of monazite M11-10 located in a garnet and one (14058) from the core of monazite M11-13 hosted in a garnet (location of grains and specimens Fig. S1).

FIB-foils for TEM were observed on a NeoARM200F Cold FEG-TEM owned by the *Consortium Lyon Saint-Etienne de Microscopie* (FED 4092) and hosted within the Hubert Curien Laboratory in Saint-Etienne. The instrument is equipped with a cold-field emission gun and with the latest generation of spherical aberration corrector on the condenser lenses. It is also equipped with a wide-angle energy dispersive X-ray (EDX) spectrometer SDD CENTURIO-X from JEOL, two scanning transmission electron microscopy (STEM) detectors (JEOL and Gatan annular dark field – ADF and JEOL annular bright field – ABF), and an electron energy-loss spectrometer EELS (Gatan GIF Quantum ER). Analyses and observations were operated at 200 kV.

APT analyses were conducted on a CAMECA Local Electrode Atom Probe (LEAP) 4000X HR hosted at the Geoscience Atom Probe Facility at Curtin University, Perth (Australia). Analyses were conducted using a UV laser (λ = 355 nm) pulsed at 125-200 kHz, a 250-300 pJ laser pulse energy, a base specimen temperature of 60 K, and an automated detection rate of 0.01 atoms/pulse (details in Tab. S1). Data processing was conducted with CAMECA's Ivas v3.8.4 and AP Suite 6 software. An evaporation field of 27.02 V/nm and an atomic average of 0.01245 nm^3/atom were used as reconstruction parameters following empirically determined parameters (Fougerouse *et al.*, 2022). ^{208}Pb/^{232}Th isotopic ratio used for dates calculation have been measured on $^{208}Pb^{2+}$ and $^{232}ThO^{2+}$ peaks at 104 Da and 124 Da

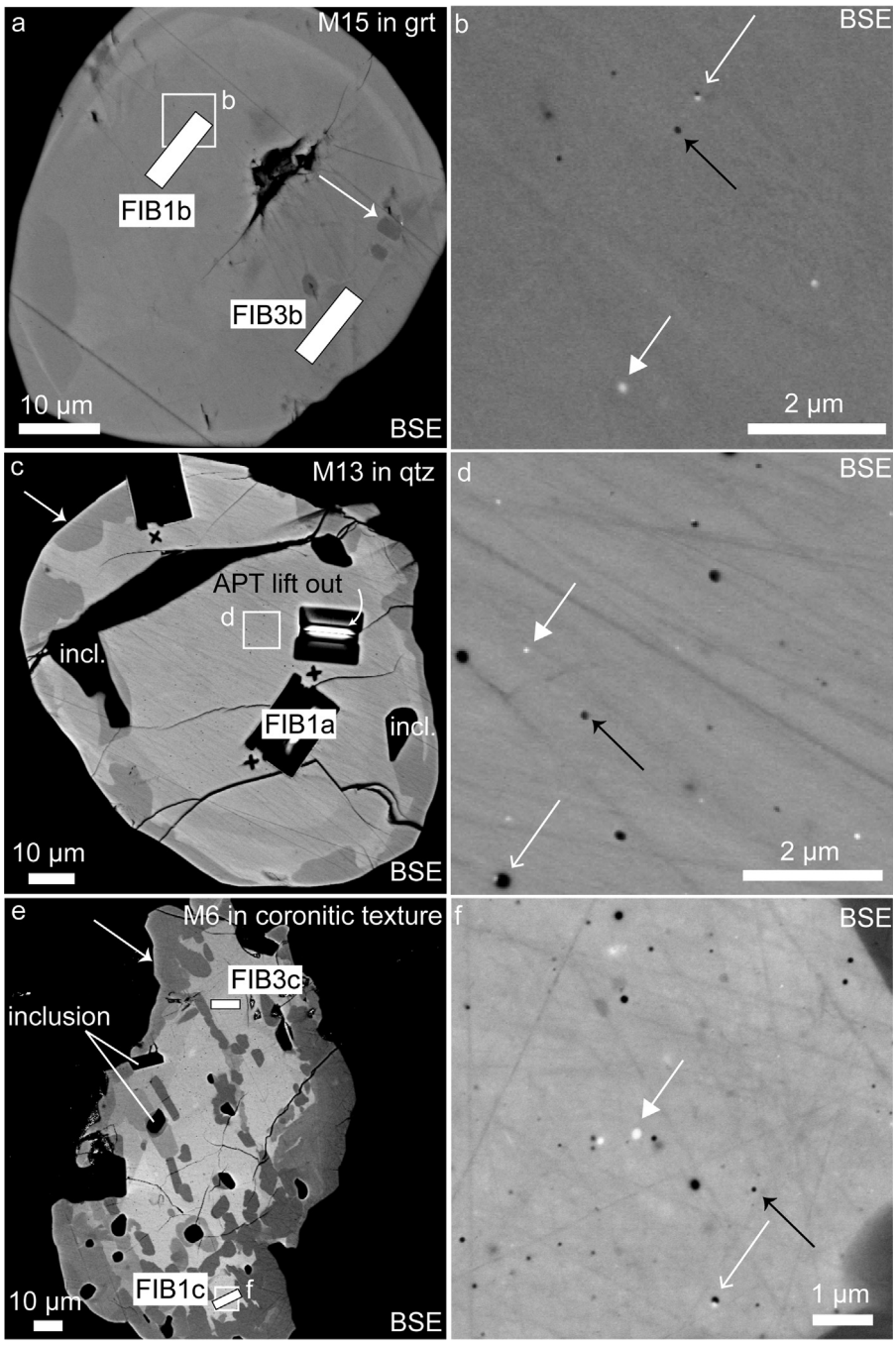

Fig. 3. BSE images of monazite grains located in garnet M15 (a, b), in quartz M13 (c, d) or in coronitic texture M6 (e, f). a: M15 grain is rounded and mostly homogeneous with localized dark contrast domains (white arrow). c: M13 is rounded, mostly homogeneous with dark contrast domains (white arrow) localized on the rim and contains silicate inclusions (incl.). e: M6 grain is anhedral with a bright core and dark contrast domains forming a rim (white arrow). Silicate inclusions are spatially associated with dark contrast domains. The three grains show the presence of nanophases corresponding to dark (black arrows) and bright (thick white arrows) spots (b, d, f) present only in cores. Some dark and bright nanophases are in equilibrium (thin white arrows).

respectively on mass spectra, using a range of 0.1 Da. Corrections procedure has been applied following Fougerouse *et al.*, (2020) recommendations. Firstly, background is measured at 100 Da for $^{208}Pb^{2+}$ and 130 Da for $^{232}ThO^{2+}$ on a peak-free area and subtracted from the counts. A correction of peak shape is then applied using the full-width at one-tenth of the maximum peak height of O_2^{2+} peak (M/ΔM10 with M the position of the maximum peak intensity and ΔM10 the full-width at tenth-maximum). For that, the software Topas is used to apply a split Pearson VII fitting with a constant background on the O_2^{2+} peak (at 31.99 Da). The O_2 M/ΔM10 is calculated at 95% confidence (2σ) and used to estimate a

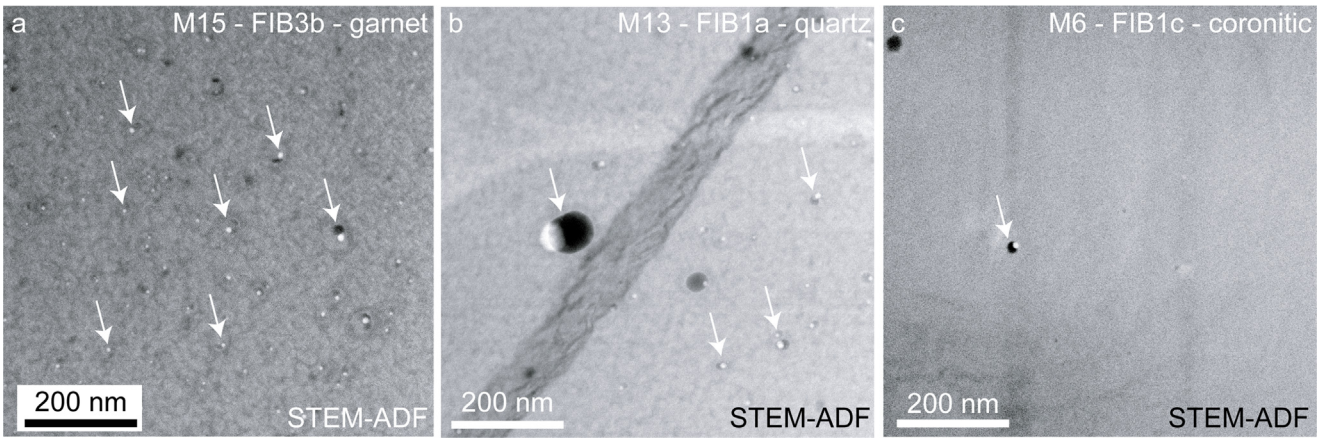

Fig. 4. STEM-ADF images of monazite hosted in garnet (a, M15–FIB3b), quartz (b, M13–FIB1a) and coronitic texture (c, M6–FIB1c). All monazite grains contain features with size < 50 nm in diameter. Features with size > 50 nm are scarce (b). Contrasting dark and bright regions indicate that features comprise two-spatially-related distinct nanophases. Imaging of M15 and M13 monazite show high number of bright nanophases (arrows) compare to monazite M6 for the same surface area.

fractioning coefficient for the peak shape. The $^{208}Pb/^{232}Th$ ratio is corrected using this coefficient.

5 Results

5.1 Textures of monazite

Our study confirms previous observations made by Goncalves (2002) that the shape of the grains depends on their petrographic position, with rounded grains mostly located in garnet and quartz (Fig. 3a and 3e). Electron backscattered images highlight density variations that arise from chemical variations within monazite grains (Fig. 3a, 3c and 3e, Fig. S2). The three grains shown in Figure 3 present light grey homogeneous cores. All monazite grains show dark contrast areas corresponding to recrystallized domains (white arrow Fig. 3a, 3c and Fig 3e), either sparsely distributed within the grain (*e.g.*, in monazite hosted in garnet, Fig. 3a) or irregular and discontinuous at grain edges (*e.g.*, in monazite hosted in quartz, Fig. 3c). In monazite grains located within the orthoamphibole and biotite coronas the dark contrast areas appear either as a large continuous rims or as euhedral domains adjacent to inclusions of quartz and biotite within the monazite grain (Fig. 3e).

Submicrometric features (Ø < 500 nm) are observed except in dark contrast domains. They appear as bright and dark contrast spots visible in high magnification BSE images (Fig. 3b, 3d and 3f). They have rounded shapes, and correspond to distinct phases within the monazite. Dark submicrometric phases contain low density material (black arrows Fig. 3b, 3d and 3f) while bright submicrometric phases contain high density material (thick white arrows Fig. 3b, Fig 3d and Fig 3f). Some bright and dark phases appear to be in textural equilibrium (thin white arrows Fig. 3b, 3d and 3f).

5.2 Nanoscale domains

STEM-ADF images from grains M15 (located in garnet), M13 (located in quartz) and M6 (located in coronitic texture), taken at the same magnification, all display bright and dark contrast spots (10–100 nm) corresponding to high- and low-density materials respectively (arrows Fig. 4). The features are circular in shape and composed by two parts highlighted respectively by dark and bright contrast spots. Most of them are 10–50 nm in diameter but scarce larger ones have 50–100 nm diameters (Fig. 4b). All features have a sharp interface with the monazite matrix (highlighted by grey contrasts) indicating that they do not represent monazite intracrystalline nanodomains but instead comprise distinct nanophases. The features are sometimes composed by two nanophases (showing bright and dark contrast respectively) which are in textural equilibrium. Monazite grains M15 and M13 hosted in garnet and quartz respectively show high concentrations of bright nanophases (~1 per 0.1 μm^2) less than 50 nm in diameter (Fig. 4a and 4b), whereas monazite M6, located in the coronitic texture, shows a very low number of bright nanophases (~1 per 0.55 μm^2, Fig. 4c). M13 and M6 monazite grains contain nanophases made of dark contrast material with size of 100–200 nm in diameters (Fig. S3).

Chemical EDS maps on a Ø > 50 nm feature composed of two nanophases located in M13 (monazite located in quartz, Figs. 4b and 5) show a marked increase in Pb concentrations in the bright part on the STEM-ADF image whereas the dark regions have higher Si concentrations (Fig. 5). Dark nanophases are generally composed of Si, Fe ± Al (Fig. S4) that are spatially decoupled.

5.3 SIMS U-Pb and APT nanogeochronology of monazite

SIMS analyses ($n = 13$) have been conducted on 10 grains (N) of monazite located in garnet ($n = 4$, $N = 3$), in quartz ($n = 3$,

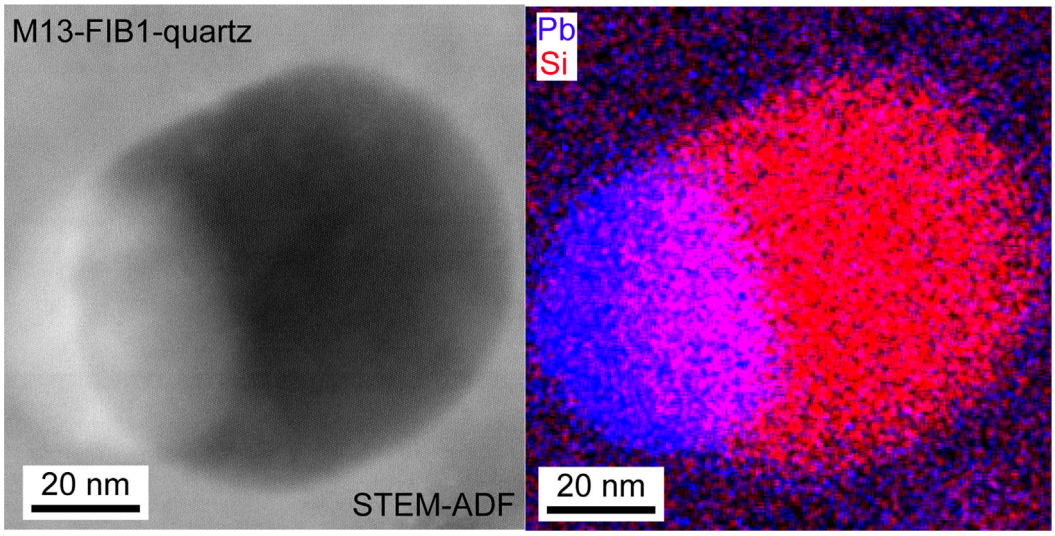

Fig. 5. Chemical EDS map obtained with TEM on a feature composed of two nanophases observed in monazite hosted in quartz (M13). Analyzed area is shown on STEM-ADF image (left) and chemical map show the spatial distributions of Pb (blue) and Si (red). Pb is strictly localized in the bright area while the darker area contains Si. The mixing area is an effect of the superposition in depth of the two nanophases (FIB foil is 50 to 100 nm thick).

$N = 2$) or in the coronitic texture ($n = 6$, $N = 5$). $^{206}Pb/^{238}U$ and $^{207}Pb/^{235}U$ isotopic data have been corrected for common Pb (Pb_c) contamination (0.02 to 13.7 ppb ^{204}Pb), which does not correlate with U-Pb discordance but is likely to be related to surface contamination during sample polishing (Tab. S2). The data are discordant and aligned along an overdispersed discordia (Fig. 6). This discordia intersects concordia at an upper intercept of 2555 ± 71 Ma (2σ) and lower intercept of 701 ± 61 Ma. The discordia obtained by selecting data only from monazite grains hosted in the UHT minerals (garnet and quartz) yields a MSWD of 1.1, an upper intercept of 2674 ± 112 Ma and an imprecise lower intercept of 1053 ± 246 Ma. Discordia obtained using data only from monazite located in the coronitic texture yields a MSWD of 1.4 when one point (Mnz1: light red on Fig. 6) is excluded, with an upper intercept at 2371 ± 160 Ma and a lower intercept at 611 ± 78 Ma. The MSWD is 4.5 if Mnz1 is included in the calculations, the resultant upper intercept being 2424 ± 496 Ma and lower intercept 653 ± 209 Ma.

Atom probe reconstruction of the specimen 3263 extracted from the monazite M13 hosted in quartz shows the heterogeneous distributions of Pb and Si atoms within the monazite (Fig. 7a). Zones of 50–100 nm in size and showing intense colour represent high atomic density areas compared to the monazite matrix, and correspond to nanophases. These nanophases may contain mostly Si (Fig. 7a, top), or both Pb and Si (Fig. 7a, bottom). Other smaller areas less than 10 nm in size and only highlighted by high Pb atom density correspond to Pb-rich clusters within monazite.

$^{208}Pb/^{232}Th$ dates have been calculated from APT specimens (3263, 3273, 14058 and 14126) lift-out in cores of monazite hosted in quartz (M13: 3263 and 3273) and garnet (M11-10: 14126 and M11-13: 14058), following the recommendations of Fougerouse *et al.* (2020) (Tab. S3). $^{208}Pb^{2+}$ and ThO^{2+} peaks are used for calculations. Analytical volumes of homogeneous monazite matrix (0.0005 μm^3) have been selected excluding, on the basis of Ivas software, all chemical heterogeneities as clusters and nanophases. Calculated isotopic ratio range between 0.050 ± 0.012 and 0.0592 ± 0.0086 corresponding to dates ranging between 987 ± 230 Ma and 1163 ± 163 Ma with a weighted mean date of 1059 ± 129 Ma (MSWD = 0.19; Fig. 7b).

5.4 LA-ICP-MS on zircon grains

LA-ICP-MS analyses on zircon ($n = 20$) have been carried out on 10 grains (N) located in garnet ($n = 3$, $N = 2$), quartz ($n = 3$, $N = 2$) or in coronitic texture ($n = 14$, $N = 6$). The $^{206}Pb/^{238}U$ and $^{207}Pb/^{235}U$ isotopic ratios show concordant to slightly discordant (17 data with discordance < 10 %) radiogenic Pb^*-loss trend (Fig. 8, Tab. S4). The $^{206}Pb/^{238}U$ concordant dates (discordance < 5 %) vary between 2432 ± 130 Ma and 2760 ± 145 Ma. The data have been sorted based on textural position. Data obtained in zircon grains hosted in garnet and quartz are concordant (discordance ≤ 5 %). A Concordia age of 2758 ± 28 Ma has been calculated from zircon hosted in garnet while those hosted in quartz yield a Concordia age of 2609 ± 51 Ma (Fig. 8). The dispersion of the dataset obtained in zircon grains located in the coronitic texture is constrained by two discordia (Fig. 8). Upper intercepts of these discordia are in good agreement with a Concordia age of 2758 ± 28 Ma obtained in zircon hosted in garnet, and with the concordant $^{206}Pb/^{238}U$ date of 2474 ± 131 Ma obtained from a zircon grain located in the coronitic texture (Fig. 8, Tab. S4).

6 Discussion

6.1 Significance of geochronological records in Andriamena unit

In the seminal case study of monazite grains from Andriamena, ID-TIMS on single monazite grains revealed four geological events at ~2700 Ma, 2523 ± 10 Ma, 738 ± 2 Ma and 576 ± 12 Ma (Fig. 2a, Paquette *et al.*, 2004). In the

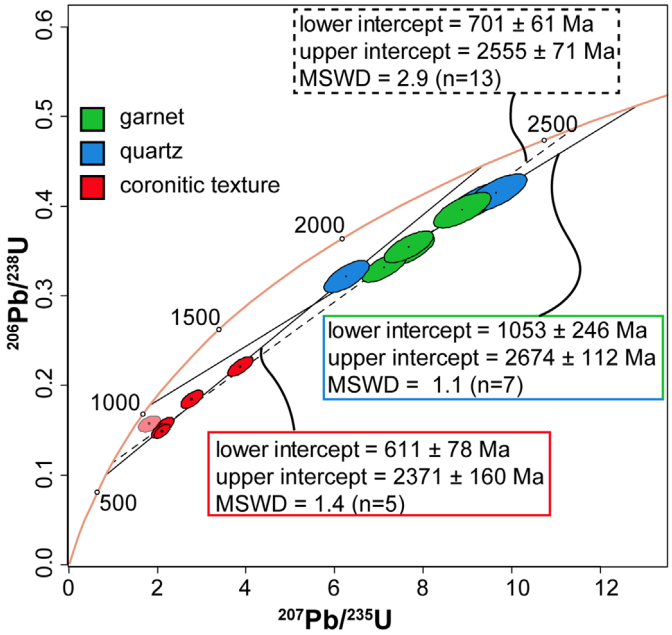

Fig. 6. Isotopic results obtained with SIMS on monazite grains. The dataset has been color coded following textural position. Uncertainties are given at 2σ. The whole dataset is discordant. Three discordia have been calculated with Isoplot software selecting the all dataset (dotted line), the data obtained in monazite located in garnet and quartz (green and blue data), the data obtained in monazite located in coronitic texture (red data) except one that follows a different trend.

following section, we will compare and discuss the new results.

The older age at ~2700 Ma of Paquette *et al.* (2004) was indicated by the upper intercept of a discordia constrained by a single large brownish monazite grain included in quartz. This age was regarded as surprising because it was unexpected that monazite affected by a protracted thermal and tectonic history, including ultra-high temperature conditions above 1000°C, could escape a total reset of the U-Th-Pb system. This ~2700 Ma event was also supported by ID-TIMS dating of zircon of granulites from the same Andriamena unit (sample C43 and C1 in Paquette *et al.*, 2004). The few other records for this age are a Rb/Sr whole-rock isochron indicating ~2700 Ma (Windley, 1996), one concordant zircon grain at 2725 ± 12 Ma interpreted as recycled xenocrystic zircon, and discordant zircon grains at 2676 ± 6 Ma with the disturbance interpreted to arise from a magmatic event recorded some 100 km north of the sampling area of this study (Kabete *et al.*, 2006). The new isotopic data on zircon grains (LA-ICP-MS) from the investigated sample An6e strengthen the evidence for a ~2700 Ma Neoarchean event, with a concordant age calculated from zircon grains hosted in garnet of 2758 ± 28 Ma. The discordia obtained in this study on monazite grains hosted in quartz and garnet indicate an upper intercept at 2674 ± 112 Ma (SIMS) that overlaps this Neoarchean event.

More varied dates have been obtained in zircon grains hosted in quartz, with a concordant analysis yielding a date of 2609 ± 51 Ma. The protolith of An6e could be a sedimentary rock resulting from the alteration of komatiite (Goncalves, 2002). Thus, the large variety of dates obtained could reflect the range of detrital sources. An alternative interpretation would be the continuous crystallisation of zircon under a UHT event lasting more than 100 My (Laurent *et al.*, 2018). Further studies are required to determine the isotopic and geological significance of this complex dataset.

The late Archean (~2500 Ma) event is also confirmed by our new results. The 2555 ± 71 Ma intercept (SIMS, Fig. 6) of the discordia calculated with the full isotopic dataset obtained on monazite is in very good agreement with intercept calculated from the 2523 ± 10 Ma ID-TIMS date of Paquette *et al.* (2004) obtained from monazite grains from the same sample. This intercept is also in agreement with other concordant dates in monazite and upper intercepts of discordant monazite measured in samples collected from the same area (ID-TIMS, sample C43 and C1 in Paquette *et al.*, 2004). In the case of zircon, which mostly records the Neoarchean event (~ 2700 Ma) in this area (Paquette *et al.*, 2004), the youngest concordant date obtained with LA-ICP-MS on a grain located in the coronitic texture is 2474 ± 131 Ma, overlapping the late Archean event.

The 611 ± 78 Ma lower intercept of the discordia defined by SIMS analyses obtained on monazite located in the coronitic texture overlaps with both lower intercepts of the ID-TIMS data at 738 ± 2 Ma and 576 ± 12 Ma. These lower intercepts do not match the ages reported in the literature at ~790 Ma and 530-500 Ma, which had been interpreted as mixing analyses reflecting minimum and maximum age estimations (Paquette *et al.*, 2004). Unfortunately, it appears that even in the present study, which employed high-resolution *in situ* isotope analysis instruments, the domains could not be analysed separately. The lower intercept of 611 ± 78 Ma obtained by SIMS is interpreted as also being the result of mixing analyses between a ~790 Ma and a 530-500 Ma component. This last age has been documented in the sample through EMP chemical dating in recrystallized domains (Paquette *et al.*, 2004). However, the ~790 Ma

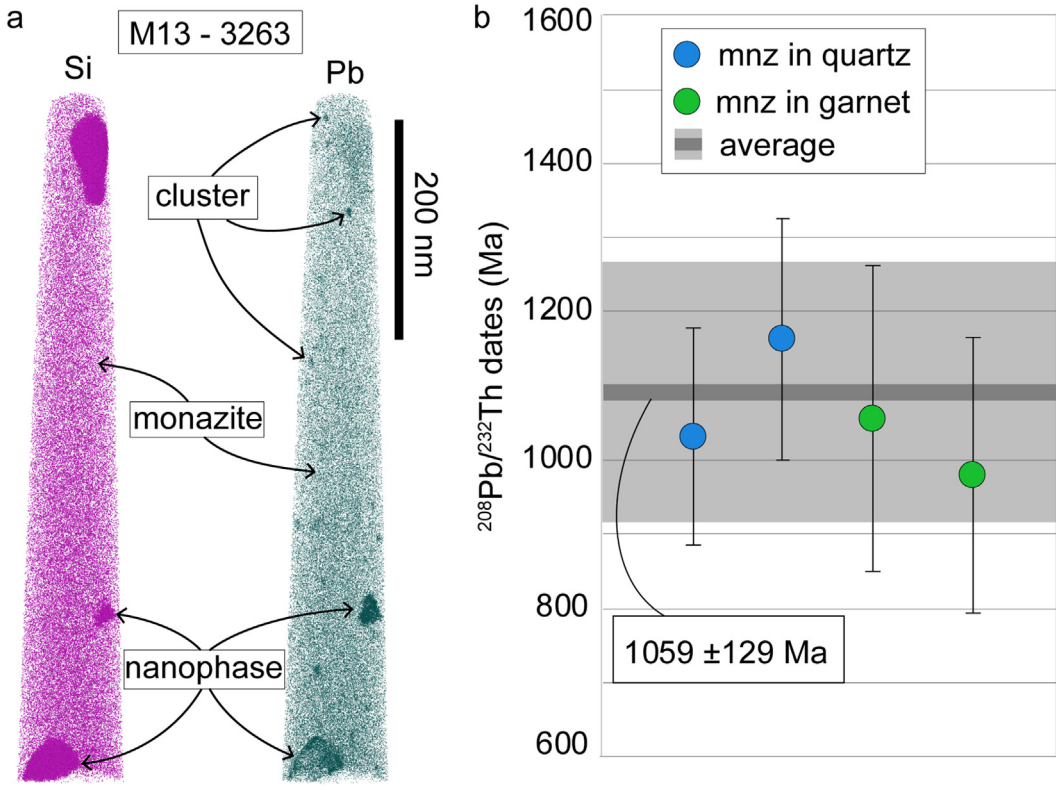

Fig. 7. Atom probe results. a: Reconstruction of atom probe specimen 3263 lifted out from the monazite M13 hosted in quartz. Pb atoms (greenish) and Si atoms (purple) distributions through the specimen are represented. One dot corresponds to one atom. Domains with intense color correspond to Pb and/or Si enrichments and highlight the presence of Pb-bearing nanophases and Si-bearing nanophases respectively. b: Atom probe $^{208}Pb/^{232}Th$ dates (uncertainties are given at 2σ) obtained in monazite located in quartz (blue) and garnet (green) avoiding nanophases. One date has been calculated for each specimen considering a volume of ~0.0005 μm^3 following Fougerouse *et al.* (2020) recommendations. The average date is 1059 ±129 Ma (2σ).

event has not been clearly documented in An6e sample as yet.

6.2 Impact of Pb-bearing nanophases in monazite on geochronological data

Nanofeatures have been recognized in monazite in billion-year-old geological contexts. These features appear in different forms, with the first recognized nanofeature, referred to as a "cluster", representing intra-crystalline domains within the monazite lattice, less than 10 nm in size, where radiogenic Pb accumulates (Seydoux-Guillaume *et al.*, 2019; Turuani *et al.*, 2023; Verberne *et al.*, 2023; Hyde *et al.*, 2024). Clusters are not recognized as having an impact on the geochronological record at the micrometer-scale. Nanophases rich in Pb, ranging in size from 10-20 nm to 1 μm (Turuani *et al.*, 2022, Turuani *et al.*, 2023 Verberne *et al.*, 2023 Hyde *et al.*, 2024), have also been observed observed in monazites from ancient geological contexts. These nanophases are always associated with nanoporosity and are therefore considered to have formed *via* dissolution-precipitation mechanism through *in situ* fluid interaction, with the prior presence of clusters being a prerequisite for their formation. A diversity of Pb-bearing nanophases has been identified, including galena (PbS) and Pb-oxides (Turuani *et al.*, 2023) and also cerussite (Hyde *et al.*, 2024). This demonstrates that the nature of the nanophases that precipitate strongly depends on the elements available within the monazite as well as any brought by the fluid. These Pb-bearing nanophases have proven to be important in preserving the record of early events within polymetamorphic samples despite the extreme conditions sometimes imposed by the later, overprinting, secondary events (Turuani *et al.*, 2022; Hyde *et al.*, 2024).

In the present sample (An6e) monazite grain cores containing variable abundances of Pb-bearing nanophases yield EMP chemical dates spread between ~700 and ~2700 Ma (Goncalves 2002; Paquette *et al.*, 2004). From the ID-TIMS results of Paquette *et al.* (2004) and the *in situ* SIMS dating of the present study it appears that monazite grains located in quartz and garnet show a lower percentage of Pb^*-loss along the discordia than monazite grains located in the coronitic textures (Fig. 6). Our nanoscale investigations reveal that the quartz- and garnet-hosted monazite grains contain a higher proportion of Pb-bearing nanophases than those now hosted in the coronitic texture (Fig. 4 and 5). This inverse correlation between the number of Pb-bearing nanophases and the percentage of Pb^*-loss has already been described for discordant monazite grains from another ancient UHT to HT

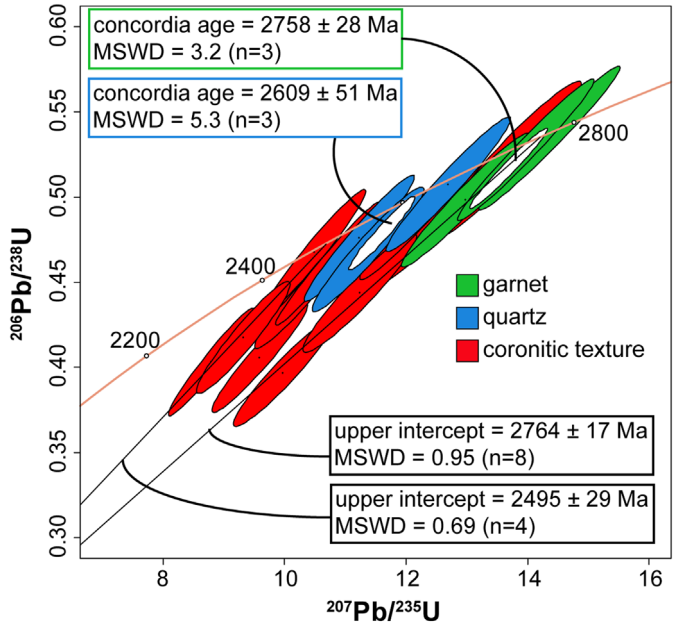

Fig. 8. Isotopic results obtained with LA-ICP-MS on zircon grains. The dataset has been color coded following textural position. Uncertainties are given at 2σ. The whole dataset is slightly discordant. Concordant dates of 2758 ± 28 Ma and 2609 ± 51 Ma have been calculated with Isoplot software from analysis obtained in zircon grains hosted in garnet (green) and quartz (blue) respectively. Due to the large dispersion of the whole dataset, two discordia have been calculated (inferior and superior limits) to bring a time constrain of the dispersion.

geological environment (Turuani *et al.*, 2022). We concur with other recent studies (Turuani *et al.*, 2023; Hyde *et al.*, 2024) which propose that the formation of Pb-bearing nanophases limits Pb^*-loss at the grain scale and therefore allows the preservation of early events.

At the nanoscale, homogeneous volumes (~$50 \times 50 \times 50\ nm^3$) of monazite that are free of Pb-bearing nanophases and located in quartz and garnet record a $^{208}Pb/^{232}Th$ age at 1059 ± 129 Ma. This age corresponds to the lower intercept of the discordia (1053 ± 246 Ma) obtained through SIMS analyses on monazite from the same textural position. This discordia also yielded an upper intercept at 2674 ± 112 Ma. Following Turuani *et al.* (2023), we suggest that these monazites crystallized at 2674 ± 112 Ma and then Pb^* accumulation in the lattice induced subsequent clusters formation. This pre-conditioned the monazite to be reactive to fluid access, which occurred at 1059 ± 129 Ma. At that time, monazite grains were affected by a coupled process consisting of (1) nanoscale resetting of the U-Th-Pb isotopic chronometers developed in the Archean monazite, and (2) the coeval precipitation of Pb^*-bearing nanophases within the monazite, favoured by the presence of clusters. This coupled process led, overall, to Pb^* retention at the scale of individual monazite grains and at typical microscale analytical volumes (Turuani *et al.*, 2023). In this scenario fluid access is limited for those monazite grains hosted in garnet and quartz. A small amount of fluid reaches monazite, enough to induce monazite dissolution and precipitation and thus reset the chronometers, but not enough to induce Pb^* leaching from the grain. Indeed, the small amount of infiltrating fluid is rapidly saturated in Pb^* inducing the precipitation of nanophases. During this process other phases may form associated with the Pb^*-bearing nanophases (Si-glass, FeS phase; Turuani *et al.*, 2023). At the grain scale, this results in limited Pb^* loss thanks to the precipitation of Pb^*-bearing nanophases, so that the more abundant the nanophases, the less discordant the isotopic record (Turuani *et al.*, 2022). In comparison, monazite grains hosted in the coronitic texture are exposed to a larger, though still limited, fluid flux, which induces greater Pb^* loss at the grain scale (Montel *et al.*, 2000; Turuani et al., 2022, 2023). The main implication of this is that conventional *in situ* dating methods operating at the micron-scale (*e.g.*, LA-ICPMS, SIMS and EMP) cannot avoid Pb^*-bearing nanophases, where present, being incorporated into the analytical volume. Mixing between ~1 Gyr monazite matrix volumes and Pb^*-bearing nanophases will then lead to discordant dates, in this example varying between 1059 ± 129 Ma and 2674 ± 112 Ma depending on the proportion of Pb^*-bearing nanophases present in the analytical volume accessed within the monazite.

6.3 New evidence for a record at Stenian-Tonian limit (Mesoproterozoic): Geodynamic setting of the 1.05 Ga event in Andriamena?

The most striking result is the calculated lower intercept at 1053 ± 246 Ma obtained based on the monazite U-Pb isotopic ratios measured with SIMS. Although the uncertainty is large, the MSWD of 1.1 indicates that the discordia is statistically well-defined. This lower intercept is consistent with the APT nanogeochronology, which yields a unimodal $^{208}Pb/^{232}Th$ average age of 1059 ± 129 Ma from monazite hosted in quartz and garnet. The low MSWD (0.19) in this case is mostly due to high uncertainties (~20%) on individual data points. Interest-

ingly, dates obtained with EMP on monazite belonging to the "UHT group" of Goncalves (2002), hosted in garnet and quartz, range continuously from Archean dates of ~2700 or ~2500 Ma down to a minimum date of ~1000 Ma (Goncalves 2002; Paquette *et al.*, 2004). Based on these three independent datasets we suggest that this late Mesoproterozoic age could represent the timing of an important but somewhat fugitive isotopic resetting event. The potential record of a Stenian event was also found in another Mg-granulite from Andriamena unit (sample C21 in Goncalves 2002), but it was neither interpreted nor considered in the geological evolution of the area. The discovery of nanodomains of Stenian age also confirms that useful geochronological information that is lacking or obscure at the microscale may be preserved in monazite at the nanoscale, adding detail to the geological evolution and potential correlations with other units and terranes (Turuani *et al.*, 2022).

The Stenian age of ca. 1 Ga identified herein is well known in the Ikalamavory unit, composed of metasedimentary and metavolcanic rocks, southwest of the Andriamena unit. The Ikalanavory unit is intruded by the acid to mafic plutonic rocks of the Dabolava Suite, dated at ca. 1 Ga (Tucker *et al.*, 2007, 2014). These intrusions have been interpreted to reflect arc magmatism (Armistead, 2019). The ca. 1 Ga dates obtained in the present study and in another granulite of the Andriamena unit (C21, Goncalves 2002) suggest that the thermal event related to this arc magmatism may be more extensive than previously thought. This new geochronological information provides an incentive for further exploration in order to better understand the geodynamic evolution of the polymetamophic tectonic basement of Madagascar.

7 Tribute to Jean-Louis Paquette – Perspectives from past to present

This contribution is a tribute to Jean-Louis Paquette's career. Jean-Louis Paquette was a worldwide known geochronologist that has largely contributed to the development and application of zircon and monazite isotopic geochronology. Since his PhD, "*Comportement des systèmes isotopiques U-Pb et Sm-Nd dans le métamorphisme éclogitique. Chaîne Hercynienne et chaîne Alpine*" defended in 1987 at the University of Rennes, Jean-Louis Paquette has published more than 200 articles, for a total of citations exceeding 10000. These papers cover a wide range of geological contexts, but some of them are related to analytical developments (Paquette *et al.*, 1994, 2003, 2004, 2014; Paquette and Tiepolo, 2007; Paquette and Pin, 2001). Jean-Louis Paquette has also largely supported the development of EMP chemical dating method in the mid-90's (Montel *et al.*, 1996). Although Jean-Louis Paquette was an isotopic geochronologist, he always recognized the benefit of this *in situ* technique to resolve geochronological problems at the micrometric scale. His experience, comments and advices, greatly helped improving the method and interpreting the results. Jean-Louis Paquette was a pioneer French researcher in the development of the LA-ICP-MS dating (Paquette *et al.*, 2007). He has also largely contributed to the characterization of monazite standards, like the famous Moacyr Brazilian monazite that has been distributed in many labs worldwide. Jean-Louis Paquette has also largely contributed to the understanding of the behavior of the U-Th-Pb isotopic system in monazite and zircon either by (1) studying unusual geochronological dataset, like the monazite grains from An6e sample, used in this contribution and coming from the PhD thesis of P. Goncalves (2002), (2) ID-TIMS dating of single grains experimentally reset (Seydoux-Guillaume *et al.*, 2002) or (3) by combining bulk, single grain and *in situ* dating techniques (Paquette *et al.*, 2004). In all these studies, Jean-Louis Paquette has played a major role through the acquisition of the isotopic data. All this tremendous work has led to cutting-edge research on nano-investigation of U, Th, Pb distribution in monazite (Seydoux-Guillaume *et al.*, 2003) and to the recent development of APT nano-geochronology (Seydoux-Guillaume *et al.*, 2019; Fougerouse *et al.*, 2020; Turuani *et al.*, 2022). Jean-Louis Paquette was also keen to improve our geological knowledge even if he had to disprove his own papers. For instance, in Paquette and Nédélec (1998), stratoid granites from North-Central Madagascar were dated with high precision at 630 Ma by isotopic dilution on multi-grain fractions of zircon. This age has embarrassed, to some extent, many geologists working in Madagascar but the quality of the data was such that these ages were seen has robust data. Almost 20 yr later, Nédélec *et al.* (2016) have performed new dating of the same samples with *in situ* LA-ICP-MS and obtained two concordant ages at 790 and 555 Ma. They concluded that the 630 Ma ID-TIMS age was not accurate but rather resulted from mixing between two zircon populations.

Finally, Jean-Louis Paquette has also mentored three of the authors of this contribution during their PhD (Marion Turuani, Anne-Magali Seydoux-Guillaume and Philippe Goncalves). He was also a collaborator of Jean-Marc Montel and Christian Nicollet when they worked all together at the laboratoire Magmas et Volcans in Clermont-Ferrand, France. With this contribution, we would like to pay a modest tribute to the tremendous and enthusiastic researcher who was Jean-Louis Paquette.

Supplementary material

Figure S1. A: BSE imaging of the location of M11-13 and M11-10 monazite grains located in garnet. B: BSE imaging of M11-13 monazite grain with location of the specimen for atom probe. C: BSE imaging of M11-10 monazite grain with location of the specimen for atom probe.

Figure S2. BSE imaging of monazite grains located in quartz (a, b) and in coronitic texture (c, d). Monazite grain located in quartz is subeuhedral and shows internal contrast variations forming a core-rim texture and contains bright and dark spots. Darker domains corresponding to recrystallized domains are present at the border of the grain. Monazite grain located in coronitic texture is anhedral and shows heterogeneous internal contrast variations with recrystallized domains at the border or near to silicate inclusion.

Figure S3. STEM-ADF images of FIB3 in M6 monazite grain located in coronitic texture (A) and FIB1a in M13 monazite grain located in quartz (B) showing nanophase filled with low-density element (dark rounded). Rounded micrometer-scale features on figure B is the holey carbon grid where FIB foil was deposited.

Figure S4. STEM-ADF image and EDS chemical map obtained with TEM on nanophase observed in FIB1a in M13 monazite grain located in quartz. Scale bars = 100 nm.

Table S1. Details on instrumentation, software, acquisition conditions, acquisition results and reconstruction parameters for APT analyses.

Table S2. Detailed results of SIMS analyses on monazite. The italic line corresponds to the excluded analysis.

Table S3. Atom probe 208Pb/232Th dates obtained in monazite hosted in quartz and garnet. Dates have been calculated for each specimen in a homogeneous volume of ∼ 0.0005 µm3.

Table S4. 206Pb/238U and 207Pb/235U ages calculated in zircon from LA-ICP-MS analyses.

The Supplementary Material is available at https://www.bsgf.fr/10.1051/bsgf/2024013/olm.

Acknowledgments

We would like to thank Clementine Fellah for assistance on SEM, Stéphanie Reynaud (LabHC) for FIB preparation for TEM, Cristina Talavera and other staff of the EIMF team for their help on SIMS analyses and Philippe de Parseval for assistance on EMP. We thank reviewers Pavel Pitra and Stéphanie Duchêne for their constructive comments which have significantly improved the manuscript. UJM and CNRS (INSU TelluS-SYSTER and IEA nanomobility) are thanked for financial support and CAMECA for access to Ivas software. We thank the CLYM for access to the TEM in Saint-Etienne (France).

References

Archibald DB, Collins AS, Foden JD, Payne JL, Holden P, Razakamanana T, *et al.* 2016. Genesis of the Tonian Imorona-Itsindro magmatic Suite in central Madagascar: insights from U-Pb, oxygen and hafnium isotopes in zircon. *Precambrian Res* 281: 312–337.

Armistead S. 2019. Tectonic evolution of Madagascar over three billion years of Earth' s history. Doctoral dissertation. University of Adelaide.

Boger SD, Hirdes W, Ferreira CAM, Schulte B, Jenett T, Fanning CM. 2014. From passive margin to volcano-sedimentary forearc: the Tonian to Cryogenian evolution of the Anosyen Domain of southeastern Madagascar. *Precambrian Res* 247: 159–186.

Bybee GM, Ashwal LD, Wilson AH. 2010. New evidence for a volcanic arc on the western margin of a rifting Rodinia from ultramafic intrusions in the Andriamena region, north-central Madagascar. *Earth Planet Sci Lett* 293: 42–53.

Fougerouse D, Reddy SM, Saxey DW, Erickson T, Kirkland CL, Rickard WDA, *et al.* 2018. Nanoscale distribution of Pb in monazite revealed by atom probe microscopy. *Chem Geol* 479: 251–258.

Fougerouse D, Kirkland CL, Saxey DW, Seydoux-Guillaume AM, Rowles MR, Rickard WDA, *et al.* 2020. Nanoscale isotopic dating of monazite. *Geostand Geoanal Res* 44: 637–652.

Fougerouse D, Cavosie AJ, Erickson T, Reddy SM, Cox MA, Saxey DW, *et al.* 2021a. A new method for dating impact events – Thermal dependency on nanoscale Pb mobility in monazite shock twins. *Geochim Cosmochim Acta* 314: 381–396.

Fougerouse, D., Reddy, S.M., Seydoux-Guillaume, A., Kirkland, C. L., Erickson, T.M., Saxey, D.W., Rickard, W.D.A., Jacob, D., and Clark, C. (2021b). Mechanical twinning of monazite expels radiogenic lead. Geology, 49, 417–421.

Fougerouse D, Saxey DW, Rickard WD, Reddy SM, and Verberne R. 2022. Standardizing spatial reconstruction parameters for the atom probe analysis of common minerals. Microscopy and Microanalysis, 28(4), 1221-1230.

Gasquet D, Bertrand J-M., Paquette J-L., Lehmann J, Ratzov G, Ascenção De , *et al.* 2010. Miocene to Messinian deformation and hydrothermalism in the Lauzière Massif (FrenchWestern Alps): new U-Th-Pb and Argon ages. *Bull Soc Géol Fr* 181: 227–241.

Goncalves P. 2002. Petrology and geochronology of ultra-high temperature granulites of the basic unit of Andriamena (north-central Madagascar). Contribution of *in situ* U-Th-Pb geochronology to the interpretation of PT paths (No. FRNC-TH-5608). Universite Blaise Pascal.

Goncalves P, Nicollet C, Lardeaux JM. 2003. Finite strain pattern in andriamena unit (north-central Madagascar): evidence for late Neoproterozoic-Cambrian thrusting during continental convergence. *Precambrian Res* 123: 135–157.

Goncalves P, Nicollet C, Montel JM. 2004. Petrology and *in situ* U-Th-Pb monazite geochronology of ultrahigh-temperature metamorphism from the Andriamena mafic unit, north −central Madagascar. Significance of a petrographical P-T path in a polymetamorphic context. *J Petrol* 45: 1923–1957.

Goncalves P, Williams ML, Jercinovic MJ. 2005. Electron-microprobe age mapping of monazite. *Am Mineral* 90: 578–585.

Guerrot C, Cocherie A, Ohnenstetter M. 1993. Origin and evolution of the west Andriamena Pan African mafic-ultramafic complexes in Madagascar as shown by UU-Pb, Nd isotopes and trace elements constraints. *Terra Abstracts* 5: 387.

Handke MJ, Tucker RD, Ashwal LD. 1999. Neoproterozoic continental arc magmatism in west-central Madagascar. *Geology* 27: 351–354.

Harley SL, Nandakumar V. 2014. Accessory mineral behaviour in granulite migmatites: a case study from the Kerala Khondalite Belt, India. *J Petrol* 55: 1965–2002. https://doi.org/10.1093/petrology/egu047.

Hyde WR, Kenny GG, Whitehouse MJ, *et al.* 2024. Microstructural and isotopic analysis of shocked monazite from the Hiawatha impact structure: development of porosity and its utility in dating impact craters. *Contrib Mineral Petrol* 179: 28. https://doi.org/10.1007/s00410-024- 02097-1.

Jackson SE, Pearson NJ, Griffin WL, Belousova EA. 2004. The application of laser ablation-inductively coupled plasma-mass spectrometry to *in situ* U-Pb zircon geochronology. *Chem Geol* 211 (1-2): 47–69.

Kabete J, Groves D, McNaughton N, Dunphy J. 2006. The geology, SHRIM P U–P b geochronology and metallogenic significance of the Ankisatra-Besakay District, Andriamena belt, northern Madagascar. *J Afr Earth Sci* 45: 87–122.

Kröner A, Hegner E, Collins AS, Windley BF, Brewer TS, Razakamanana T, *et al.* 2000. Age and magmatic history of the Antananarivo block, central Madagascar, as derived from zircon geochronology and ND isotopic systematics. *Am J Sci* 300: 251–288.

Kusiak MA, Dunkley DJ, Wirth R, Whitehouse MJ, Wilde SA, Marquardt K. 2015. Metallic lead nanospheres discovered in ancient zircons. *Proc Natl Acad Sci* 112: 4958–4963.

Laurent AT, Bingen B, Duchene S, Whitehouse MJ, Seydoux-Guillaume AM, Bosse V. 2018. Decoding a protracted zircon

geochronological record in ultrahigh temperature granulite, and persistence of partial melting in the crust, Rogaland, *Norway. Contrib Mineral Petrol* 173: 1–25. https://doi.org/10.1007/s00410-018- 1455-4

Ludwig KR. 2003. User's manual for Isoplot 3.00—A geochronological toolkit for Microsoft excel. Berkeley Geochronology Centre Special Publications 4.

Martelat JE, Lardeaux JM, Nicollet C, Rakotondrazafy R. 2000. Strain pattern and late Precambrian deformation history in southern Madagascar. *Precambrian Res* 102: 1–20.

Montel JM, Foret S, Veschambre M, Nicollet C, Provost A. 1996. Electron microprobe dating of monazite. *Chem Geol* 131 (1-4): 37–53.

Montel JM, Kornprobst J, Vielzeuf D. 2000. Shielding effect of garnet for the U-Th-Pb system in monazite: example from the Beni-Bousera kinzigites (Morocco). *J Metamorph Geol* 18: 335–342.

Nédélec A, Paquette JL, Antonio P, Paris G, Bouchez JL. 2016. A-type stratoid granites of Madagascar revisited: age, Source and links with the breakup of Rodinia. *Precambrian Res* 280: 231–248.

Nicollet C. 1988. Métabasites granulitiques, anorthosites, et roches associées de la croute inférieure – Exemples pris à Madagascar et dans le Massif Central français. Thèse d'Etat, Université Blaise Pascal (Clermont-Ferrand, France). https ://theses.hal.science/tel-00787525

Paquette JL, Nédélec A, Moine B, Rakotondrazafy M. 1994. U-Pb, single zircon Pb-evaporation, and Sm-Nd isotopic study of a granulite domain in SE Madagascar. *J Geol* 102 (5): 523–538.

Paquette JL, Nédélec A. 1998. A new insight into Pan-African tectonics in the East-West Gondwana collision zone by U-Pb zircon dating of granites from central Madagascar. *Earth Planet Sci Lett* 155 (1-2): 45–56.

Paquette JL, Pin C. 2001. A new miniaturized extraction chromatography method for precise U-Pb zircon geochronology. *Chem Geol* 176 (1-4): 311–319.

Paquette JL, Moine B, Rakotondrazafy MA. 2003. ID-TIMS using the step-wise dissolution technique *versus* ion microprobe U-Pb dating of metamict Archean zircons from NE Madagascar. *Precambrian Res* 121 (1-2): 73–84.

Paquette JL, Goncalves P, Devouard B, Nicollet C. 2004. Micro-drilling ID-TIMS U-Pb dating of single monazites: a new method to unravel complex poly-metamorphic evolutions. Application to the UHT granulites of Andriamena (North-Central Madagascar). *Contrib Mineral Petrol* 147: 110–122.

Paquette JL, Tiepolo M. 2007. High resolution (5 μm) U-Th-Pb isotope dating of monazite with excimer laser ablation (ELA)-ICPMS. *Chem Geol* 240: 222–237.

Paquette JL, Piro JL, Devidal JL, Bosse V, Didier A, Sannac S, *et al.* 2014. Sensitivity enhancement in LA-ICP-MS by N2 addition to carrier gas: application to radiometric dating of U-Th-bearing minerals. *Agilent ICP-MS J* 58: 4–5.

Peterman EM, Reddy SM, Saxey DW, Snoeyenbos DR, Rickard WDA, Fougerouse D, *et al.* 2016. Nanogeochronology of discordant zircon measured by atom probe microscopy of Pb-enriched dislocation loops. *Sci Adv* 2.

Piazolo S, La Fontaine A, Trimby P, Harley S, Yang L, Armstrong R, *et al.* 2016. Deformation-induced trace element redistribution in zircon revealed using atom probe tomography. *Nat Commun* 7 (1): 10490.

Rasolomanana E, Andriamirado LC, Randrianja R, Ratefiarimino A. 2010. Analyse et interprétation des données aéromagnétiques et spectrométriques de la région d'Andriamena. *Madamines* 1: 1–14

Rickard WD, Reddy SM, Saxey DW, Fougerouse D, Timms NE, Daly L, et al. 2020. Novel applications of FIB-SEM-based ToF-SIMS in atom probe tomography workflows. Microscopy and Microanalysis, 26(4), 750–757.

Seydoux-Guillaume AM, Paquette JL, Wiedenbeck M, Montel JM, Heinrich W. 2002. Experimental resetting of the U-Th-Pb systems in monazite. *Chem Geol* 191 (1-3): 165–181.

Seydoux-Guillaume AM, Goncalves P, Wirth R, Deutsch A. 2003. Transmission electron microscope study of polyphase and discordant monazites: site-specific specimen preparation using the focused ion beam technique. *Geology* 31: 973–976.

Seydoux-Guillaume AM, Bingen B, Paquette JL, Bosse V. 2015. Nanoscale evidence for uranium mobility in zircon and the discordance of U-Pb chronometers. *Earth Planet Sci Lett* 409: 43–48.

Seydoux-Guillaume AM, Fougerouse D, Laurent AT, Gardés E, Reddy SM, Saxey DW. 2019. Nanoscale resetting of the Th/Pb system in an isotopically-closed monazite grain: a combined atom probe and transmission electron microscopy study. *Geosci Front* 10 (1): 65–76.

Tang L, Pan M, Tsunogae T, Takamura Y, Tsutsumi Y, Rakotonandrasana NOT. 2018. Cordierite-bearing granulites from Ihosy, southern Madagascar: Petrology, geochronology and regional correlation of suture zones in Madagascar and India. *Geosci Front* 10 (6): 2007–2019.

Tucker RD, Ashwal LD, Handke MJ, Hamilton MA, Le Grange M, Rambeloson RA. 1999. U-Pb geochronology and isotope geochemistry of the Archean and proterozoic rocks of north-central Madagascar. *J Geol* 107: 135–153.

Tucker RD, Kusky TM, Buchwaldt R, Handke MJ. 2007. Neo-proterozoic nappes and superposed folding of the Itremo Groupe, west-central Madagascar. *Gondwana Res* 12: 356–379. https://doi.org/10.1016/j.gr.2006.12.001.

Tucker RD, Roig JY, Moine B, Delor C, Peters SG. 2014. A geological synthesis of the Precambrian shield in Madagascar. *J Afr Earth Sci* 94: 9–30.

Turuani MJ, Laurent AT, Seydoux-Guillaume AM, Fougerouse D, Saxey D, Reddy SM, *et al.* 2022. Partial retention of radiogenic Pb in galena nanocrystals explains discordance in monazite from Napier Complex (Antarctica). *Earth Planet Sci Lett* 588: 117567.

Turuani MJ, Seydoux-Guillaume AM, Laurent AT, Reddy SM, Harley SL, Fougerouse D, *et al.* 2023. Nanoscale features revealed by a multiscale characterisation of discordant monazite highlight mobility mechanisms of Th and Pb. *Contrib Mineral Petrol* 178 (5): 1–21.

Utsunomiya S, Palenik CS, Valley JW, Cavosie AJ, Wilde SA, Ewing RC. 2004. Nanoscale occurrence of Pb in an Archean zircon. *Geochim Cosmochim Acta* 68 (22): 4679–4686.

Valley JW, Cavosie AJ, Ushikubo T, Reinhard DA, Lawrence DF, Larson DJ, *et al.* 2014. Hadean age for a post-magma-ocean zircon confirmed by atom-probe tomography. *Nat Geosci* 7 (3): 219–223.

Verberne R, Reddy SM, Saxey DW, Fougerouse D, Rickard WDA, Plavsa D, *et al.* 2020. The geochemical and geochronological implications of nanoscale trace-element clusters in rutile. *Geology* 48 (11): 1126–1130.

Verberne R, Reddy S, Fougerouse D, Seydoux-Guillaume AM, Saxey D, Rickard W *et al.*, 2024. Clustering and interfacial segregation of radiogenic Pb in a mineral host–inclusion system Tracing two-stage Pb and trace element mobility in monazite inclusions in rutile. *Am Mineral*. https:// doi.org/10.2138/am-2023-9085.

Vermeesch P. 2018, IsoplotR: a free and open tool box for geochronology. *Geosci Front* 9: 1479–1493. https://doi.org/10.1016/j.gsf.2018.04.001.

Verberne R, van Schrojenstein Lantman HW, Reddy SM, Alvaro M, Wallis D, Fougerouse D, et al. 2023. Trace-element heterogeneity in rutile linked to dislocation structures: Implications for Zr-in-rutile geothermometry. Journal of Metamorphic Geology, 41(1), 3–24.

White LF, Darling JR, Moser DE, Reinhard DA, Dunlop J, Larson DJ *et al.*, 2018. Complex nanostructures in shocked, annealed, and metamorphosed baddeleyite defined by atom probe tomography. *Microstruct Geochronol: Planet Records down to Atom Scale* 351–367.

Whitehouse MJ, Kusiak MA, Wirth R, Ravindra Kumar GR. 2017. Metallic Pb nanospheres in ultra-high temperature metamorphosed zircon from southern India. *Mineral Petrol* 111: 467–474. https://doi.org/10.1007/s00710-017-0523-1.

Windley BF. 1996. The Madagascar-India connection in a Gondwana Framework. Gondwana Research Group Mem, 3, 25–37.

Cite this article as: Turuani MJ, Seydoux-Guillaume A-M, Laurent AT, Fougerouse D, Harley SL, Reddy SM, Goncalves P, Saxey DW, Michaud J, Montel J-M, Nicollet C, Paquette J-L. 2024. From ID-TIMS U-Pb dating of single monazite grain to APT-nanogeochronology: application to the UHT granulites of Andriamena (North-Central Madagascar), *BSGF - Earth Sciences Bulletin* 195, 18.